Comparative Adsorptive Performance of Clinoptilolite, Purolite, and Mesoporous Carbon (CMK-3) for Heavy Metals and Hydrocarbons Removal from Real Petrochemical effluent / Original Article

Assist. Lact. Eynas Muhamad Majeed[1]*,

Assist. Lact. Nuha Muhsen Ali[2]

12 , Middle Technical University, Polytechnic College of Engineering Specializations, Baghdad/Iraq

*** Corresponding Author: inas.mohammed@mtu.edu.iq**

مقارنة أداء الامتزاز للكلينوبتيلوليت والبورووليت والكربون المسامي (CMK-3) لإزالة المعادن الثقيلة والهيدروكربونات من المخلفات البتروكيماوية الحقيقية

م.م ايناس محمد مجيد[1]، م.م نهى محسن علي[2]

2،1 الجامعة التقنية الوسطى، كلية البوليتكنك للتخصصات الهندسية-بغداد، بغداد\العراق

Abstract

Petrochemical activities result in the generation of effluent that contain highly toxic heavy metals and oil products, which are very hazardous to the environment. The research tries to examine the adsorption capacity of three materials synthetic clinoptilolite, synthetic Purolite, and synthesized mesoporous carbon (CMK-3) in the removal of Ni^{2+}, Cd^{2+}, Pb^{2+}, benzene, and toluene present in real refinery effluent obtained at Al-Dora Refinery in Iraq (Baghdad). The experiments were carried by batch adsorption that investigated the equilibrium behavior, kinetic performance, and the influence of ionic strength and organic co-contaminants. The heavy metal adsorption was higher in Clinoptilolite and Purolite reaching an efficiency of more than 90%. Although CMK-3 is not a good metal remover, it proved to possess high toluene and benzene removal capacity because of high surface area and mesoporous structure. Co-contaminant experiments indicated that benzene increased Pb^{2+} adsorption which could be as a result of Pbbenzene complexation and Ni^{2+} and Cd^{2+} adsorption decreased. Hydrocarbons were characterized by a two-stage isotherm model pointing to multilayer adsorption behaviour. The paper offers comparative perspectives on adsorbent performance with actual petrochemical discharge and suggests that new ways of adsorption amplification or inhibition can be offered under co-contaminant conditions.

Keywords: Mesoporous materials, Mesoporous Carbon, Clinoptilolites, Purolites, Adsorption, Heavy metals, hydrocarbon.

المستخلص

تؤدي الأنشطة البتروكيميائية إلى توليد نفايات سائلة تحتوي على معادن ثقيلة شديدة السمية ومشتقات نفطية، مما يشكل خطراً جسيماً على البيئة. يهدف هذا البحث إلى دراسة قدرة الامتزاز لثلاث مواد – الكلينوبتيلوليت الاصطناعي، والبورواليت الاصطناعي، والكربون المسامي المصنّع (CMK-3) – في إزالة أيونات النيكل (Ni^{2+})، والكادميوم (Cd^{2+})، والرصاص (Pb^{2+})، والبنزين، والتولوين الموجودة في نفايات سائلة حقيقية مأخوذة من مصفاة الدورة في العراق (بغداد). أُجريت التجارب باستخدام الامتزاز الدفعي لدراسة سلوك التوازن، والأداء الحركي، وتأثير القوة الأيونية والملوثات العضوية المصاحبة. كان امتزاز المعادن الثقيلة أعلى في الكلينوبتيلوليت والبورواليت، حيث بلغت كفاءتهما أكثر من 90%. على الرغم من أن الكربون المسامي المصنّع (CMK-3) ليس فعالاً في إزالة المعادن، إلا أنه أثبت قدرة عالية على إزالة التولوين والبنزين نظراً للمساحة السطحيه الكبيرة وبنيته المسامية. أشارت تجارب الملوثات المصاحبة إلى أن البنزين يزيد من امتزاز أيونات الرصاص (Pb^{2+})، وهو ما قد يعزى إلى تكوين معقدات مع البنزين، بينما ينخفض امتزاز أيونات النيكل (Ni^{2+}) والكادميوم (Cd^{2+}). وتم توصيف الهيدروكربونات باستخدام نموذج امتزاز ثنائي المراحل، مما يشير إلى سلوك امتزاز متعدد الطبقات. تقدم هذه الورقة البحثية منظورًا مقارنًا لأداء المواد المازة مع مخلفات البتروكيماويات الفعلية، وتقترح طرقًا جديدة لتعزيز أو تثبيط الامتزاز في ظل ظروف الملوثات المصاحبة.

الكلمات المفتاحية: المواد متوسطة المسام، الكربون متوسط المسام ، كلينوبتيلوليت، بيورواليت، امتزاز، معادن ثقيلة، هيدروكربونات.

1. Introduction

The high rate of industrialization and release of harmful substances into the river systems in an uncontrolled manner has really led to water pollution crisis globally. It has been estimated that about 80 percent of the world population experience threats of water security caused by the worsening water quality [1,2]. The energy sector, mainly, the refining of oil and natural gas, as well as the extraction of gas, contribute to this theme on a large scale by creating vast quantities of produced water. This effluent is present in solid form and is usually co-produced with oil and gases in the subsurface formations, and the mixture usually consists of complex organic and inorganic effluent. The geological particularity of the reservoir, its maturity, and the technology of obtaining water affect the particular composition of produced water. Oil to water ratios range between 2 and 3 in most parts of the globe with highest records being 50 [3].

Petrochemical operations normally produce and process waters containing a broad variety of pollutants such as dissolved metals (e.g. Pb^{2+}, Ni^{2+}, Cd^{2+}), organic hydrocarbons (e.g. benzene and toluene), residual process chemicals, oils and in some systems, naturally occurring radioactive materials (NORMs). Contamination by ground water can also be through poor management of these effluent or through the leachings in contaminated soils [4]. Some treatment technologies including the pump-and-treat (P&T) systems and the permeable reactive barriers (PRBs) have been suggested to treat such contaminated waters both above as well as in situ. These structures depend on the chemical conversion, microbial decomposition, or immobilization by adsorption to degrade the number of pollutants [5].

Specifically, adsorption has been known to be efficient in the removal of organic and inorganic contaminants because it is simple, cost effective and can be adapted to different matrices of water. Heavy metals were also successfully adsorbed onto such

materials as synthetic zeolites and ion-exchange resins (Purolite) due to their strong affinity in binding divalent metal ions such as Pb^{2+}, Cd^{2+}, and Hg^{2+} [6].

These materials however tend to perform poorly in the treatment of complicated effluents that have both organic and inorganic compounds or in the event of high ionic strength like salty waters [7].

The recent trend of research has directed to the usage of mesoporous carbon adsorbents like CMK-3 and CMK-8 on the basis of their special structure, big pore volumes and high specific surface areas that may rise above 1000 m^2/g. These materials are unusually hydrophobic and are highly capable of 1-1 interactions; they are therefore well suited to the adsorption of non-polar and aromatic organic chemicals, such as benzene and toluene [8,9] Moreover, these high-temperature stable mesoporous carbons can be easily reactivated by application of mild heat or solvents, when compared to many carbands-based materials, which are unstable during acidic and/or high-temperature treatments.

Mesoporous carbon has higher performance, in terms of removal of hydrophobic pollutants in presence of co-existing metal ions, as compared to using mesoporous silica. That renders them perfect fits to deal with complicated industrial effluents, like, oil refinery effluents. Cyclic structure with ordered mesopores with templating CMK - 3 carbone makes the CMK - 3 capable of multilayer adsorption and capillary condensation, both of which lead to high adsorption of volatile and semi-volatile organic compounds [10].

In the present paper we have tested the efficiency of synthetic clinoptilolite, synthetic Purolite and mesoporous carbon (CMK - 3) in removal of heavy metals (Pb^{2+}, Cd^{2+} and Ni^{2+}) and organic pollutants (benzene and toluene) in real petrochemical effluent in Al-Dora Refinery located at Baghdad, Iraq. To study the equilibrium behavior, kinetics and the effect of the ionic strength and co-contaminant

interference, adsorption experiments were carried out. The comparative study gives mechanistic information regarding the adsorption behavior of both materials and points out the benefits of using the mesoporous carbon in the cleaning of mixed-contaminant industries effluents.

2. Materials and Methods

2.1 Materials

CMK - 3 mesoporous carbon was prepared by hard-templating of CMK - 3 with CMK - 3 as a carbon precursor according to [11]. Unreacted furfuryl alcohol was carbonized at 900 C in nitrogen atmosphere and the template was removed by etching with 10 % HF. The product material possessed a surface area of 1240 m^2 /g, 3.9 nm pore diameter, and pore volume of 1.3 cm^3/g.

Synthetic clinoptilolite and Purolite resins are purchased in the commerce. These two were cleaned with deionized water and exchanged with NaCl (2M) to make sure that uniform presence of Na^+ existed in the exchange sites.

2.2 Effluent source and characterization

The actual effluent used was a sample that was taken at the Al-Dora Refinery (Baghdad, Iraq), which was filtered to get rid of suspended solids. The first measurements of the amount of benzene and toluene were 400-600 mg/L, whereas heavy metals (Ni^{2+}, Pb^{2+}, Cd^{2+}) were 0.9-1.5 mg/L.

2.3 Batch adsorption tests

The experiments were carried out in 250 mL conical flasks with the amount of 50 mL of pollutant solution and 0.05 g of adsorbent mixed at 150 rpm temperature of 25 ^oC. Kinetics were observed at each 24 hours. The concentration of hydrocarbons

was determined on Shimadzu TOC-CSV analyzer and heavy metals with ICP-OES (Vista MPX, Varian).

2.4 Isotherm and model fitting

The adsorption data was applied on Langmuir, Freundlich, and Langmuir Freundlich models. As already proposed by [12] using mesoporous media, the two-step adsorption of benzene and toluene was fitted with a hybrid isotherm as a combination of Langmuir and Langmuir Freundlich terms.

3. Results and discussion

3.1 Kinetics of adsorption: heavy metals

Pb^2, Cd^2, and Ni^2 adsorption kinetics onto clinoptilolites, Purolites, and CMK-3 are depicted in Figures 1-3 correspondingly. Rapid adsorption kinetics and high elimination of every metal were noted. Table 1 displays the parameters derived from the nonlinear regression using the pseudo-first order model Eq. (1), each of which is accompanied by the standard error value. The regression process determined the standard error for the adjustable parameters Ce and Kobs, while the measured parameter C0 served as the reference for the instrumental precision.

$$\frac{dC}{dC} = k_{obs}(C - C_e) \qquad \textbf{(1)}$$

For both Purolites and Clinoptilolites, the kobs value was comparable for every metal tested, indicating minor variations in each adsorption rate. When it came to removing heavy metals, the Purolites and Clinoptilolites outperformed the CMK-3. The zeolite and Purolites reached an equilibrium condition in 100 minutes, whereas the CMK-3 took 200 minutes to reach the same state. Nonetheless, as evidenced by the strong Pearson coefficient (R^2) value, the model well captured the kinetics of the chosen heavy metal adsorption process.

3.2 Adsorption isotherms for heavy metals: Purolites and Clinoptilolites

The target heavy metals' adsorption isotherm onto the Purolites and natural zeolite (clinoptilolites) is displayed in Figures 4-6. With the exception of Pb^2 adsorption onto clinoptilolites (which showed an inflection point in the lower concentration range), it can be observed that the suggested following model Eq. (2) fit the Purolites and clinoptilolites adsorption data quite well.

$$q_e = \frac{1}{2}\left[\frac{2K_{Na}+.q_{\max}.Ce+1}{K_{Na}+.Ce}\right] - \sqrt{\frac{4K_{Na}+.q\max.Ce+1}{(K_{Na}+.Ce)^2}} \qquad \textbf{(2)}$$

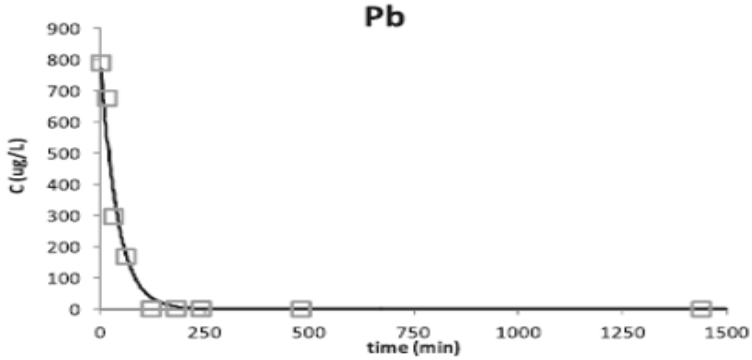

(a) Purolites

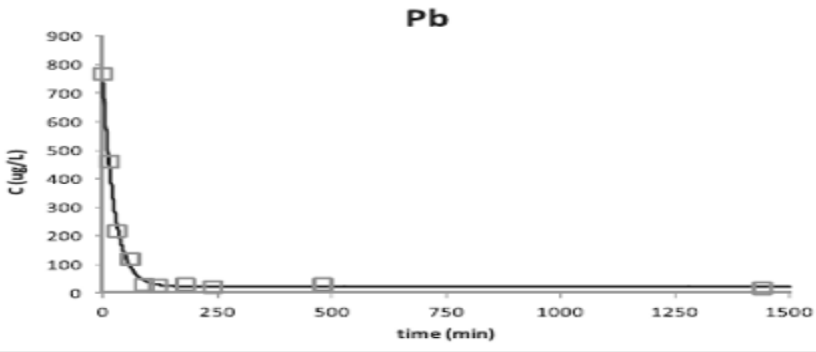

(b) Clinoptilolites

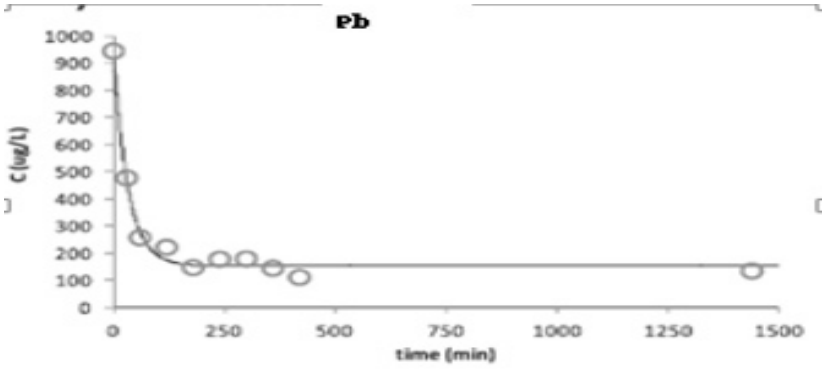

(c) CMK-3

Figure 1. Pb^2 adsorption kinetics onto.

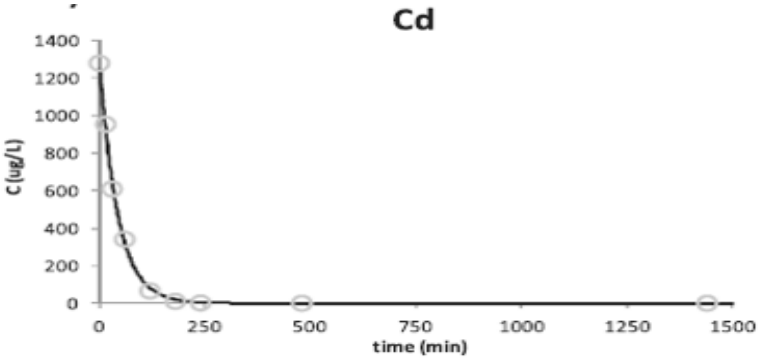

(a) Purolites

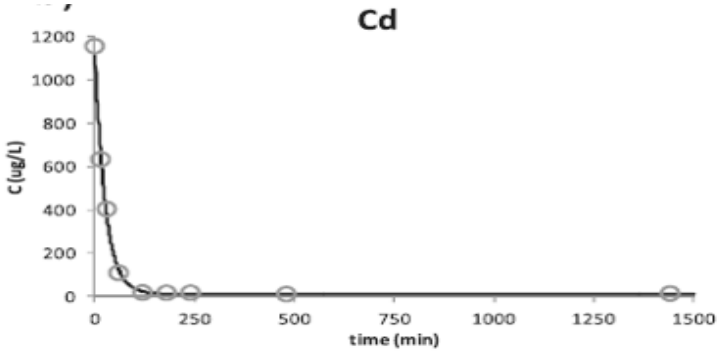

(b) Clinoptilolites

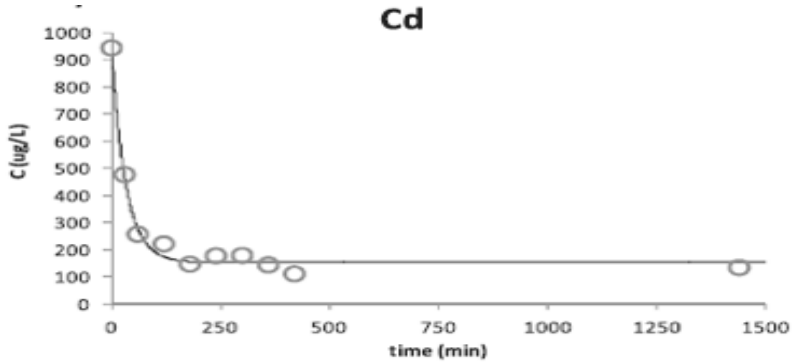

(c) CMK-3

Figure 2. The adsorption kinetics of Cd^2 onto.

The zeolite surface's heterogeneity was cited as the reason for this distinct behaviour. It is commonly recognized that, like other naturally occurring carbon, surface structures suggest that the clinoptilolites surface is distinguished by the regenerated material has both ion exchange (a permanent negative charge resulting from the isomorphic substitution of Si4 with Al3) and complexation sites (open hydroxyl active functional groups) [13]. Thus, this surface eOH may open up one additional avenue in the adsorption of metals (Pb^2, Cd^2, and Ni^2).

In connection with this, it has been demonstrated earlier that Pb^2 ions are capable of forming more stable hydroxo-complexes than Cd^2 or Ni^2 ions [14], which can perhaps partly explain the fluctuations in Pb adsorption activity. While adsorption into the complexation sites will be active for all of the metals, only Pb^2-type will show massive adsorption in low ionic strength. Since the created model (2) only involved single adsorption mechanism, it did not capture clinoptilolites Pb^2 adsorption in this case. On the other hand, the Purolites was only characterized by the presence of chelating sites, and the model did capture/ explain the behaviour of the experiments. The Langmuire-Freundlich model therefore quantified the Pb^2

adsorption behaviour, given that surface heterogeneity was incorporated by the mathematical formulation.

This is the equation that represents the Langmuir Freundlich isotherm [15]:

$$q_e = q_{\max} \frac{K.(Ce)^b}{1 + K.(Ce)^b} \quad \textbf{(3)}$$

where Ce is the equilibrium solution concentration in mg/L, K is the equilibrium constant in L/g, b is the maximum adsorbable amount in mg/g, qe is the quantity of Pb^2.

heterogeneity is a parameter that has been quantified using the symbol is. This isotherm was more applicable to account for the lead's heterogeneous adsorption process on clinoptilolites [16]. The characteristic values of the and clinoptilolites isotherms based on the optimized parameters are presented in Table2 and statistical parameters of the goodness of fit. The adsorbed quantity of Pb^2.

is a parameter for heterogeneity. This isotherm was more suited to explain the lead's heterogeneous adsorption mechanism onto clinoptilolites [17]. The optimized parameters for the and clinoptilolites isotherms are shown in Table 2, along with statistical parameters that show the goodness of fit.

A slight lower value for the Cd^2 as compared to Ni^2 and Pb^2 the resulted depicted that there was no tremendous variation in the affinity constant between chosen heavy metals in the Purolite. These results indicated that each of the four amidoximes had a stability in relation to the heavy metals that were almost proportionate.

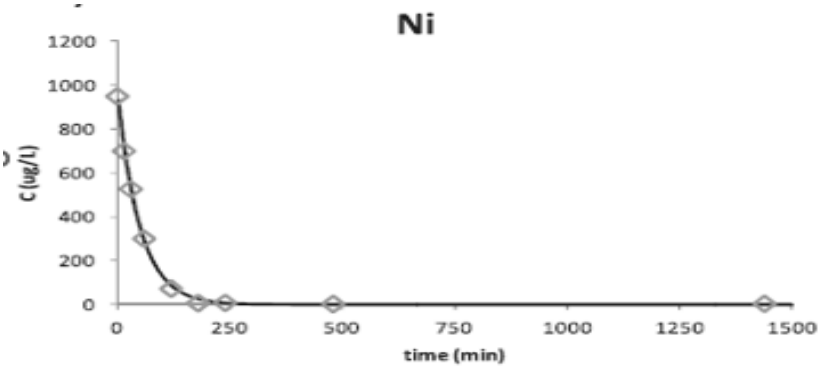

(a) Purolites

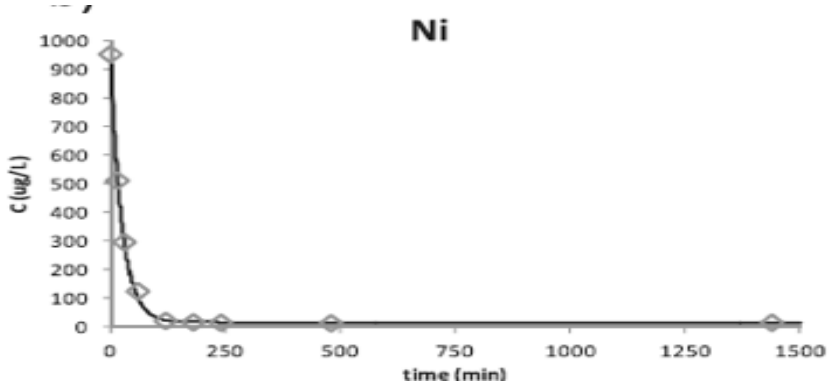

(b) Clinoptilolites

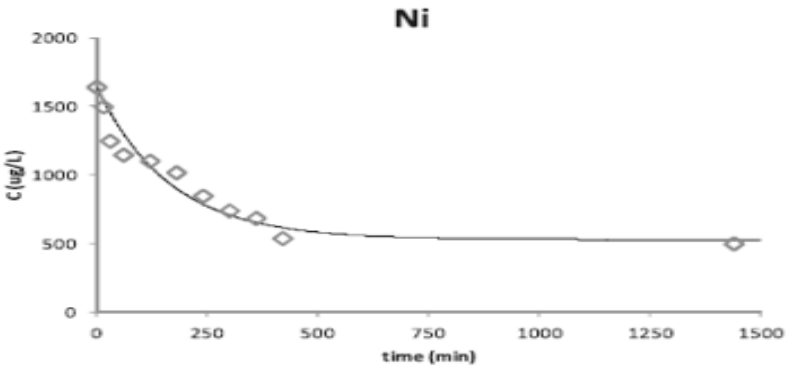

(c) CMK-3

Figure 3. Kinetics of Ni^2 adsorption onto.

Table 1. Ni^2, Cd^2, and Pb^2 adsorption kinetic parameters were optimised for Clinoptilolites, CMK-3, and Purolites.

		Ce (mg/L)	K (min-1)	Co (mg/L)	R2
Clinoptilolites	Pb^{2+}	**11.74 ±16.90**	**0.0234±0.004**	**713±45**	**0.902**
	Cd^{2+}	**105 ± 28**	**0.0215±0.0037**	**1172±25**	**0.971**
	Ni^{2+}	**16.2 ± 3.1**	**0.0308±0.001**	**967±38**	**0.914**
Purolites	Pb^{2+}	**(2.91 ± 0.35)E-18**	**0.0251±0.003**	**763±22**	**0.981**
	Cd^{2+}	**(3.45 ± 0.38)E-7**	**0.0245±0.021**	**1053±35**	**0.95**
	Ni^{2+}	**(1.56 ± 0.6)E-18**	**0.0311±0.0045**	**942±42**	**0.904**
CMK-3	Pb^{2+}	**530 ± 312**	**0.0035±0.018**	**1378±31**	**0.917**
	Cd^{2+}	**105 ± 28**	**0.0178±0.0049**	**2082±47**	**0.995**
	Ni^{2+}	**451.1 ± 235.9**	**0.0047±0.0061**	**1835±55**	**0.962**

3.2.1 Ionic strength's effect

As seen from Figures 7-9, experimental isotherms of the adsorption of Ni^2, Pb^2, and Cd^2 onto Purolites and clinoptilolites.

relative to the behaviour that the computations predicted when measured with high degrees of ion strength. However, as the metal concentrations decreased, the adsorption shape was different, and all the metal isotherms in the clinoptilolites case here showed the same behaviours. If competition from the high Na concentration inhibited the adsorption of Ni^2 and Cd^2 at ion exchange sites at higher ionic strengths, the contribution of adsorption to complexation sites became relatively significant, which could account for this. These theories were in line with a better clarified Ni^2 and Cd^2 isotherm execution.

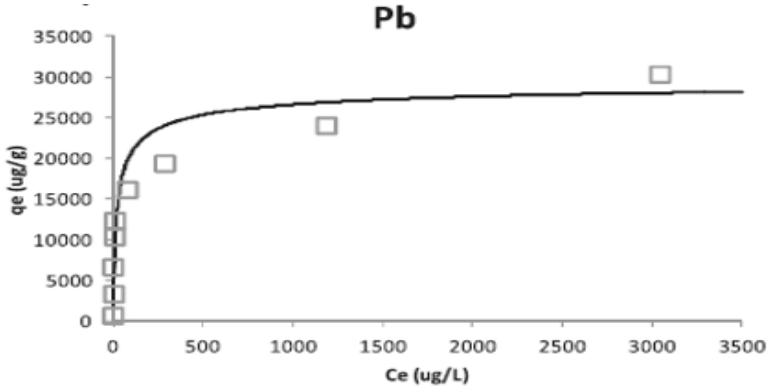

(a) Purolites

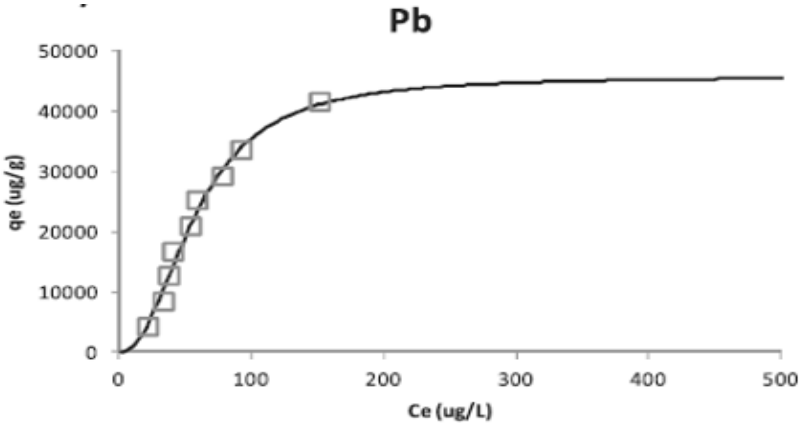

(b) Clinoptilolites

Figure 4. Pb2 adsorption isotherm onto

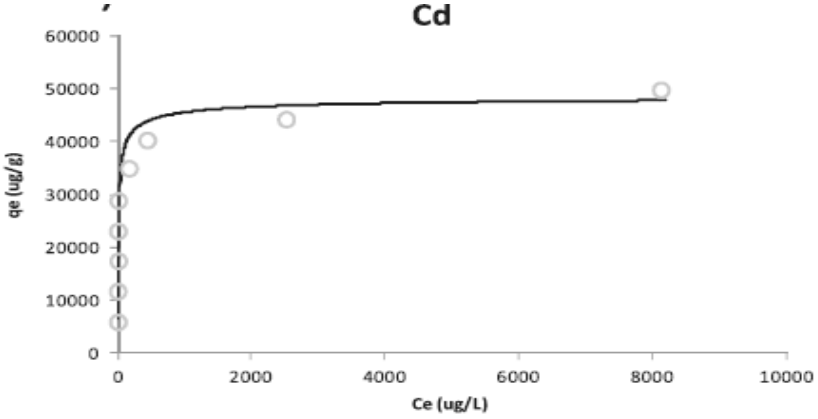

(a) Purolites

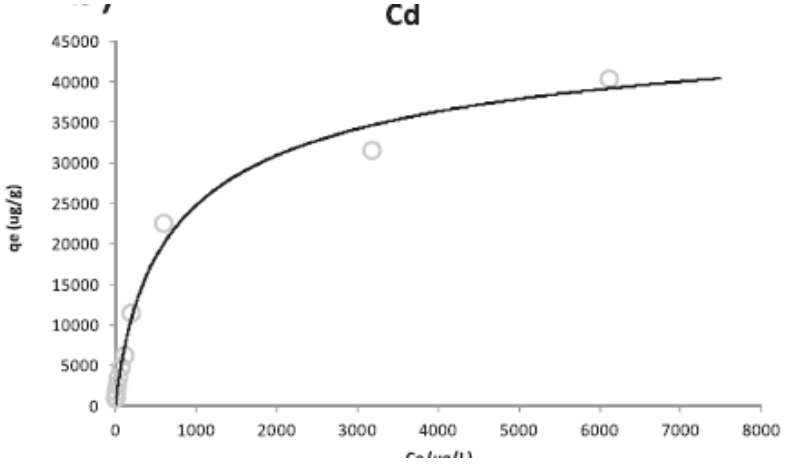

(b) Clinoptilolites

Figure 5. Cd^2 adsorption isotherm onto

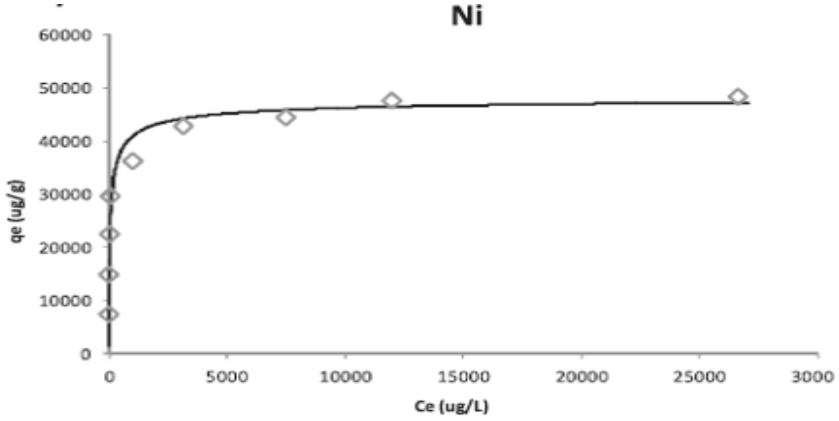

(a) Purolites

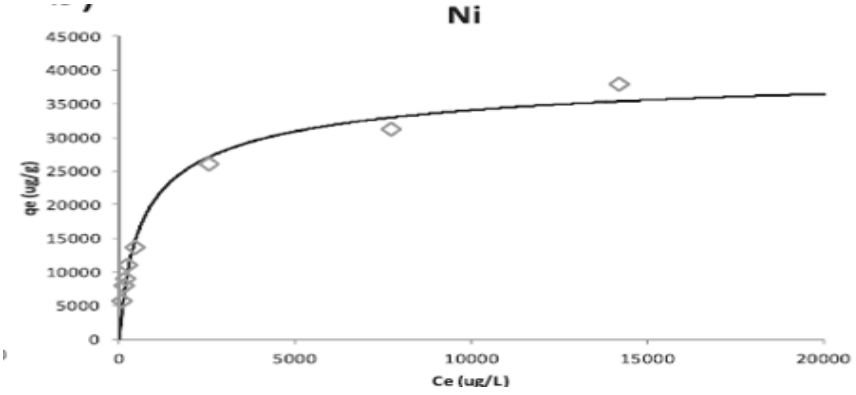

(b) Clinoptilolites

Figure 6. Comparison of the estimated and experimental behaviour for the adsorption isotherm of Ni^2 onto

Table 2. Pb^2, Cd^2, and Ni^2 adsorption onto Purolites and clinoptilolites were optimised using isotherm parameters

	Purolites			Clinoptilolites		
	Ni^2	Pb^2	Cd^2	Ni^2	Pb^2	Cd^2
qmax (ug/g)	43,000 ± 2400	61,000 ± 3100	44,000 ± 1400	50,000 ± 2200	34,000 ± 2600	30,900 ± 2100
KNa^+ or K (L/g)	(2.94 ± 0.621) E-08	0.017 ± 0.001	(3.21 ± 0.592) E-08	(2.86 ± 0.592) E-08	(4.04 ± 0.) E-08	(2.86 ± 0.592) E-08
b	--------	--------	--------	--------	2.25 0.217	--------
R^2	0.981	0.901	0.975	0.922	0.974	0.954

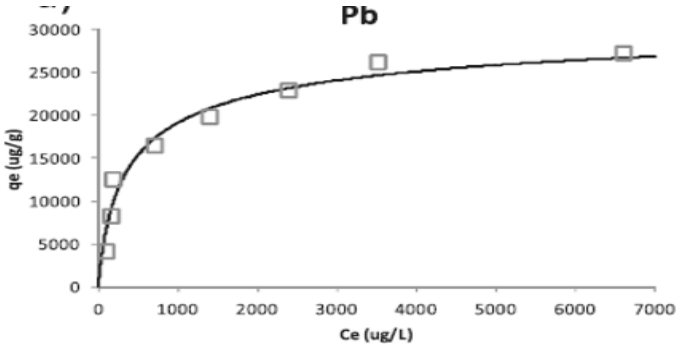

(a) Purolites

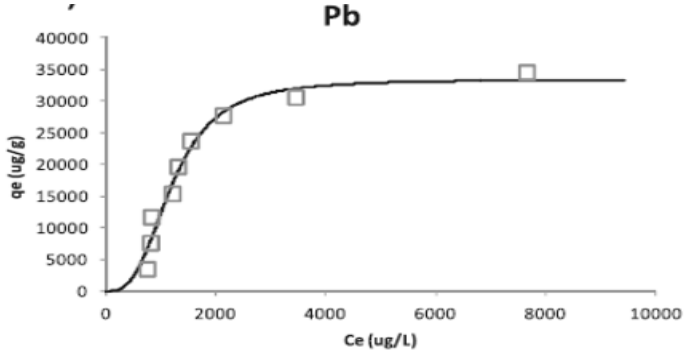

(b) clinoptilolites at high ionic strength

Figure 7. Comparison of estimated and experimental behaviour for Pb^2 isotherm onto.

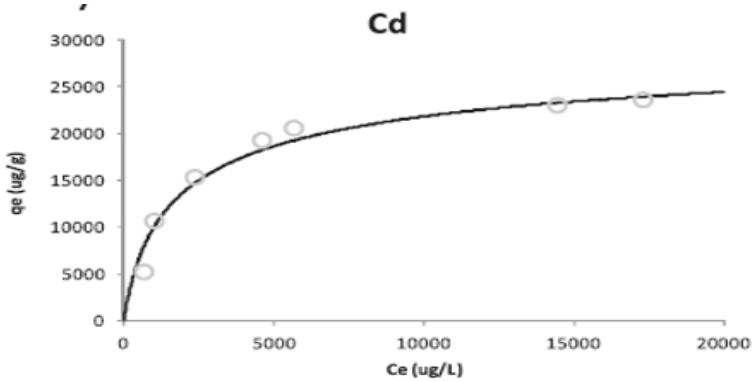

(a) Purolites

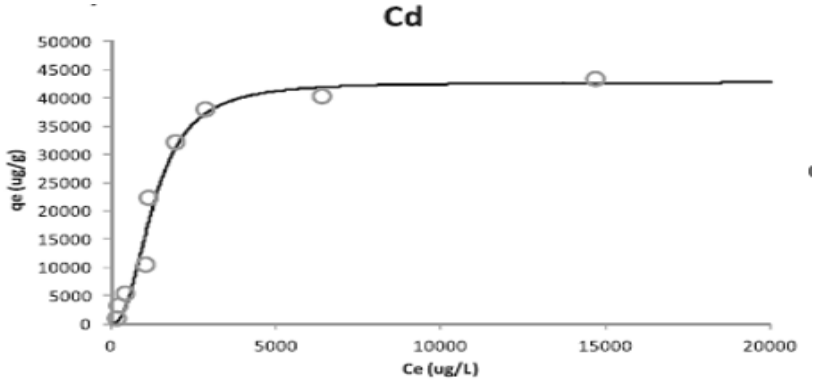

(b) clinoptilolites at high ionic strength

Figure 8. Comparison of predicted and experimental behaviour for the Cd^2 isotherm onto

represented by Eq. (3). In the instance of Pb^2, the optimized parameters demonstrated a drop in the affinity constant and qmax value, suggesting that Ni and Pb2 are in competition for the exchange sites. Regarding

the adsorption onto Purolites, model (2) remained appropriate for data representation, and no alterations in the adsorption behaviour were noted with regard to low ionic strength circumstances. Actually, there was just one adsorption site typology identified for the Purolites, and the ion

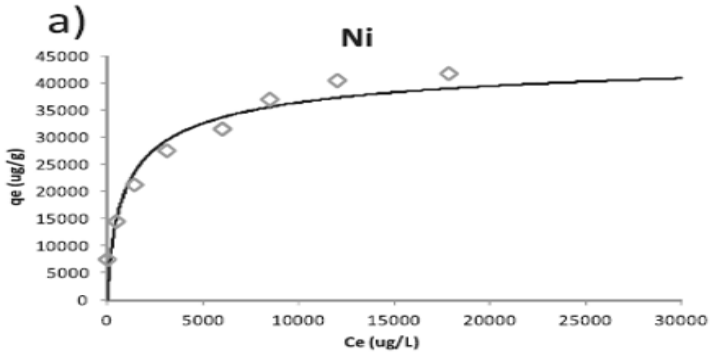

(a) Purolites

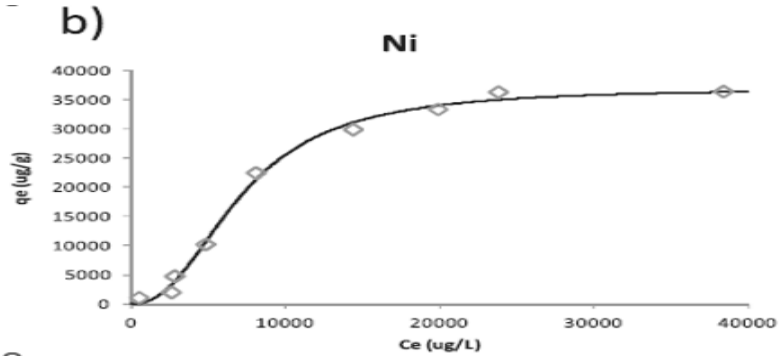

(b) clinoptilolites at high ionic strength

Figure 9. Comparison of predicted and experimental behaviour for the Ni^2 isotherm onto

Table 3. Ni^2, Cd^2, and Pb^2 adsorptions onto Purolites and clinoptilolite at high ionic strength were optimised using isotherm parameters.

	Purolites			Clinoptilolites		
	Ni^2	Pb^2	Cd^2	Ni^2	Pb^2	Cd^2
qmax (ug/g)	33,000 ± 1500	52,000 ± 2500	38,000 ± 1600	45,000 ± 1700	30,000 ± 2500	28,000 ± 2300
KNa^+ or K (L/g)	(2.21± 0.422) E-08	(3.50 ± 0.411) E-08	(3.082 ± 0.367) E-08	(4.32 ± 0.573) E-08	(6.53 ± 0.362) E-08	(4.05 ± 0.471) E-08
b	--------	--------	--------	2.25 ± 0.51	2.31 ± 0.49	2.12 ± 0.44
R^2	0.961	0.912	0.948	0.934	0.985	0.966

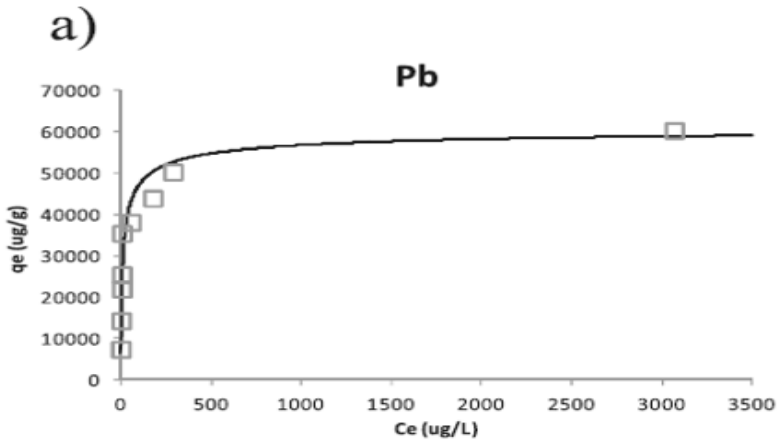

(a) Purolites

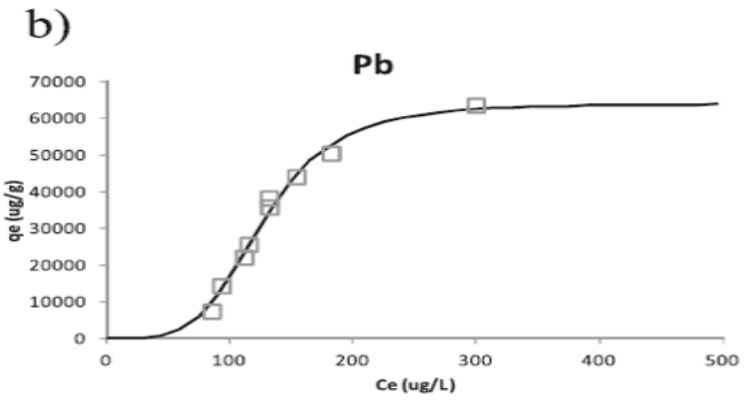

(b) Purolites with benzene present

Figure 10. Pb^2 isotherm onto

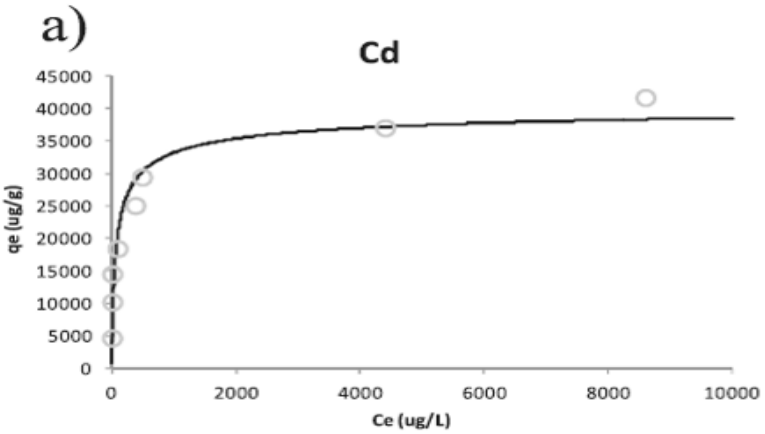

(a) Purolites

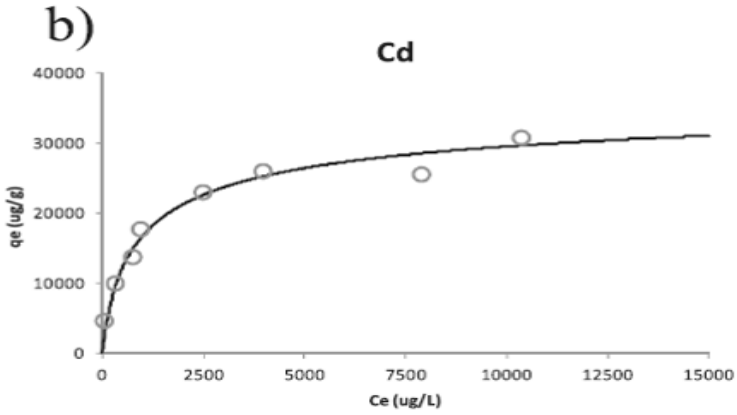

(b) Clinoptilolites with benzene present

Figure 11. Cd^2 isotherm onto

Competition only had an impact on the adsorption capacity; it had no influence on the adsorption mechanism.

The optimized values of KNa validated these findings.

as well as qmax (Table 3). The affinity and maximum adsorbable quantity of each heavy metal were found to slightly decrease when compared to the comparable values

at low ionic strength (Table 2). In fact, Na's competition for chelating sites with Pb^2, Cd^2, and Ni^2 was typically restricted to causing a notable drop in KNa and qmax values.

3.2.2 Co-contamination's effects: organic compounds

Figures 10-12 at about 500 mg/L show the adsorption isotherm of each metal ion onto each adsorbent's material in presence of benzene. It appeared that the presence of benzene had varying effects on the adsorption mechanism depending on the specific ion. The maximum adsorbable amount of Pb^2 for both Purolites and Clinoptilolites increased significantly in the presence of benzene. On the other hand, Ni^2 and Cd^2 decreased the maximum

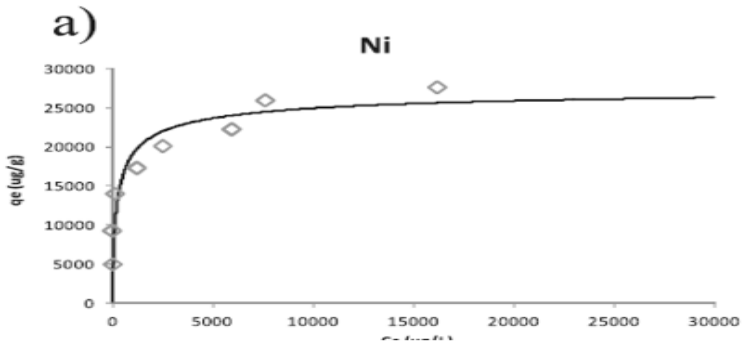

(a) Purolites

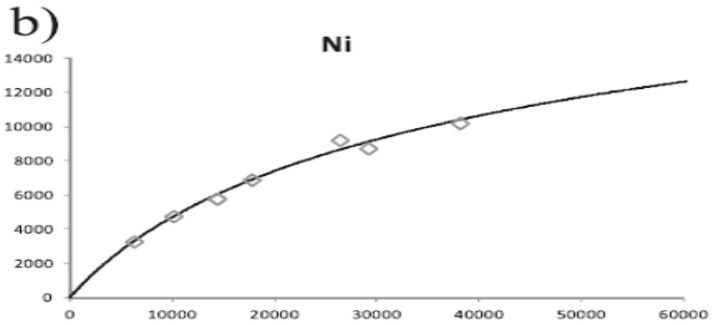

(b) Clinoptilolites when benzene is present.

Figure 12. The Ni^2 isotherm onto.

Table 4. Ni^2, Cd^2, and Pb^2 adsorption onto Purolites and clinoptilolites with optimised isotherm parameters in the presence of benzene.

	Purolites			Clinoptilolites		
	Ni^2	Pb^2	Cd^2	Ni^2	Pb^2	Cd^2
qmax (ug/g)	43,000 ± 2500	62,000 ± 3400	29,000 ± 2300	37,000 ± 2800	64.000 ± 2600	25,000 ± 1900
KNa^+ or K (L/g)	(2.31± 2.11) E-08	(2.44 ± 3.16) E-08	(3.24 ± 1.50) E-08	(8.41 ± 2.53) E-08	0.0091 ± 0.0003	(3.72 ± 1.04) E-08
b	--------	--------	--------	--------	3.91 ± 0.57	--------
R^2	0.925	0.943	0.928	0.914	0.935	0.926

only a minor impact on the affinity constants, and an adsorbable quantity for both adsorbents (refer to Table 4).

To have a better understanding of the various ways that benzene affects metals adsorptions, benzene concentrations fluctuation during the adsorptions testing was tracked by taking measurements at the start and finish of each trial as shown in Figures13-15. Despite the fact that the experimental results were very dispersed, Pb^2 showed distinct behaviour in comparison to Cd^2 and Ni^2. Regardless of the rise in the initial metal concentration, Benzene retention in the Pb2 trials was frequently higher. According to reports.

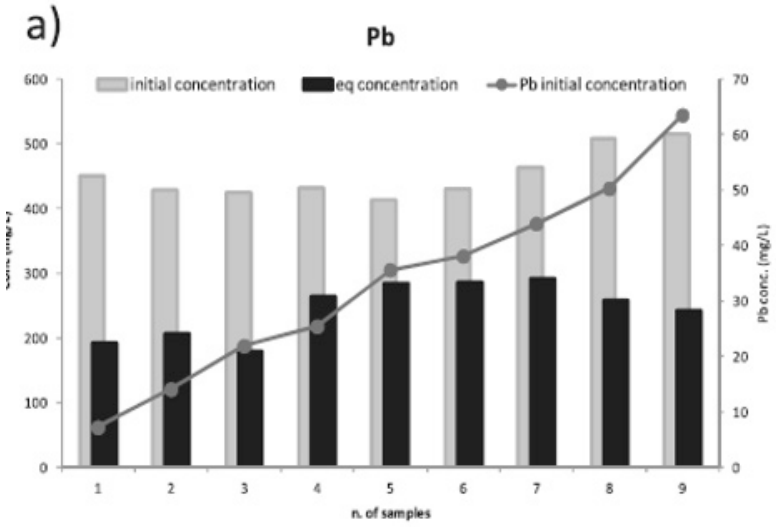

(a)

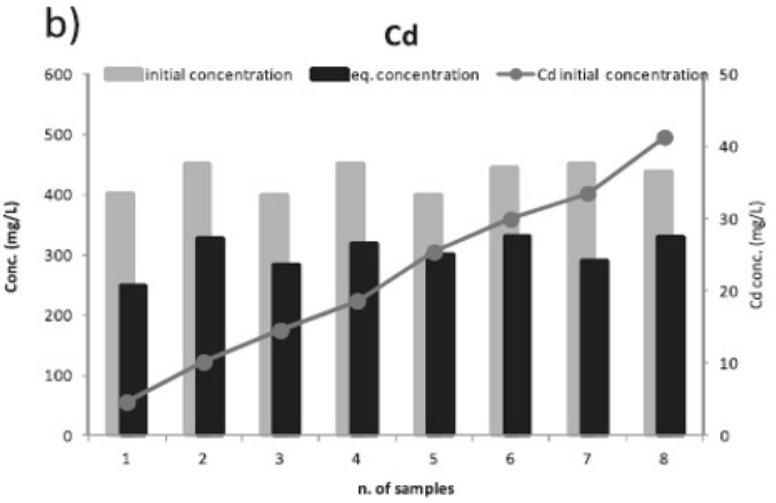

(b)

Figure 13. a) Cd^2-Purolites and, (b) Cd^2-clinoptilolites adsorption test alterations in benzene content before (grey) and after (black).

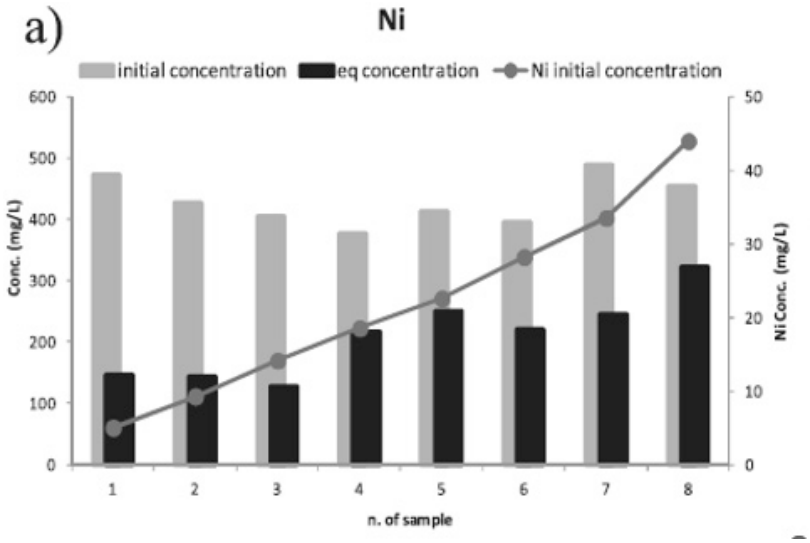

(a) Ni^2/Purolites

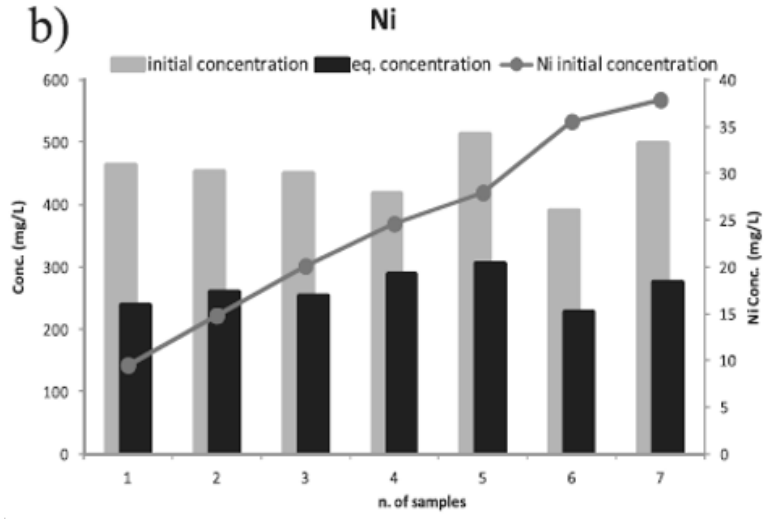

(b) Ni2-clinoptilolites adsorption procedure

Figure 15. Benzene concentrations variation before (grey) and after (black).

Figure 16. shows the adsorption isotherms of Pb and Cd onto CMK-3 which exhibit that lead more adsorbed onto CMK-3 than cadmium.

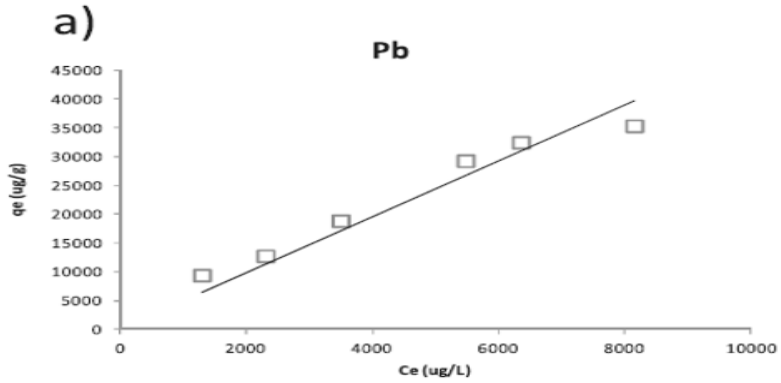

(a)

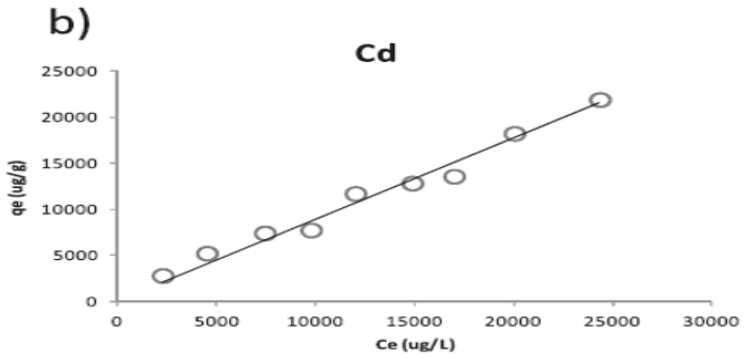

(b)

Figure 16. Cd^2 and Pb^2 adsorptions isotherms onto CMK-3.

in the scholarly literature [18] Pb^2 can form stable complexes with benzene molecules, which may elucidate the observed favorable impact on its adsorption. Conversely, no information was located.

about the possible complexation of benzene with Cd^{2+} and Ni^{2+} in research. Our experimental results suggested that the simultaneous adsorption of Pb^2 ions

and benzene Pb-complex (general formula [Pb(C6H6) x]2) onto the selected adsorbents may improve the adsorption of Pb^2.

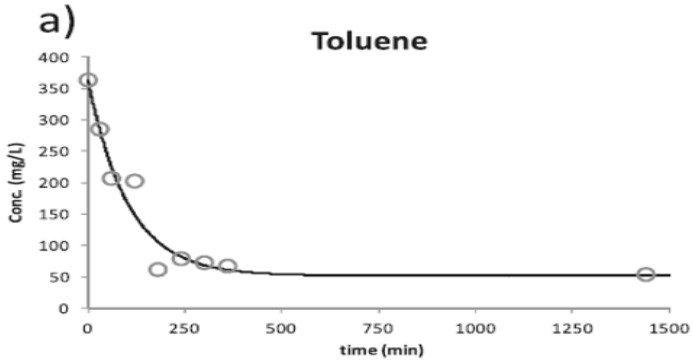

(a)

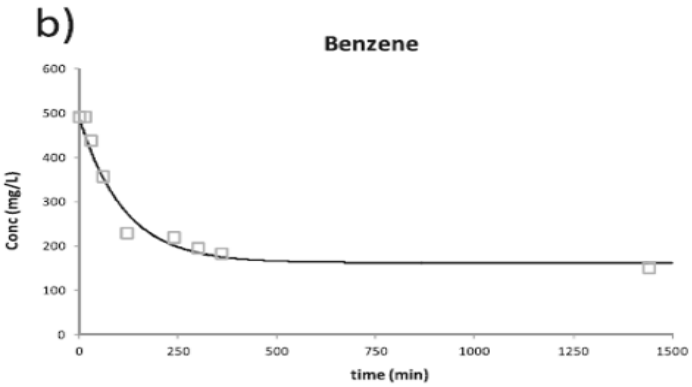

(b)

Figure 17. Benzene and Toluene adsorption kinetics onto CMK-3.

3.3 Isotherms for heavy metals adsorptions: CMK-3

Figure 16 shows the experimental results of adsorption of the target heavy metals Pb^2 and Cd^2 onto CMK-3. Different from clinoptilolites. Within the specified testing range, the adsorption isotherm for purolites showed linear behaviour and a significantly lower removal capacity. This isotherm of the Henry type is commonly used to represent the adsorption process at low solute concentrations and/or low surface affinities (and hence minimal surface coverage) [19]. Alumina's role as a binder in the CMK-3 's bulk structure may have contributed to the observed adsorption by offering more suitable adsorption sites for the removal of heavy metals. Given that the CMK-3 is possessing forms with generally low affinity, the low metal removal capability was in line with this [20]. Purolites and Clinoptilolites appeared to be better and better adapted for heavy metal uptake, and the CMK-3's efficacy in eliminating heavy metals was not comparable to theirs, even with alumina present.

3.4 Removal of hydrocarbons

3.4.1 Kinetics of adsorption: organic substances

These hydrocarbons are benzoene and toluene the most prevalent hydrocarbons and are in huge quantities in the produced goods [21]. Due to this relevance the two were used as sample hydrocarbon indicators of water contamination.

From the experimental data and using Eq (1) the estimated dependence of the kinetics of benzene and toluene adsorption on the CMK-3 layer is represented in Figure 17. In connection with Eq. (1), the optimized parameters are listed in Table 5, which results from the nonlinear regression analysis of the experimental data. The pseudo-first order kinetic equation given above was used. (1) once again provided a useful analogue for characterizing the rate of adsorption when the two hydrocarbons had stabilized at equilibrium after 6 – 7 hours. Also, upon analyzing

the exponential decay of the offered CMK-3and the benzene content after 24h contact time, the toluene decrease offered extra evidence that CMK-3 had enhanced benzene absorption capability.

3.4.2 Adsorption isotherm for hydrocarbons: CMK-3

Experimental adsorption isotherms of toluene and benzene on CMK-3 are plotted in Figure 18. The nature of the experimental results was consistent with a two-stage adsorptive process whereby there was significant deviation from a pure Langmuir isotherm model at low concentrations, indicated by a shift in the nature of the isotherms. This type of experimental form has been noted earlier for the adsorption of organic contaminants from gaseous phase onto mesoporous materials [21] but there has been no report for adsorption of dissolved organics from solution. Hence, the results of the experimental isotherms were modeled using the hybrid isotherm model, developed for the first time in the work of [22]. The isotherm consists in the first part of the behaviour of the experimental points by the Langmuir equation and in the second part by the Langmuire Freundich isotherm.

The first part of the experimental behaviour was explained by the Langmuir equation, and the second part by the Langmuire Freundlich isotherm. The expression for this model. The optimized kinetic parameters for the adsorption of benzene and toluene onto CMK-3 are presented in Table 5.

Table 5. Optimized kinetics for adsorptions of toluene and benzene onto CMK-3.

Parameters	Benzene	Toluene
C0 (mg/L)	471 ± 22	380±14
kobs (min^{-1})	0.0081 ±0.0042	0.0091 ± 0.0050
Ce (mg/L)	172 ± 11	64 ± 16
R^2	0.953	0.921

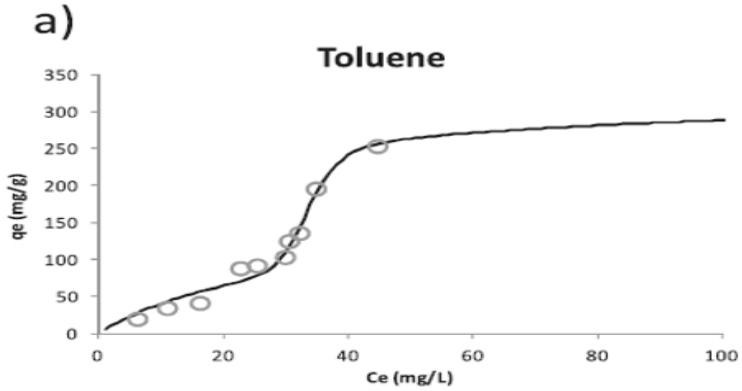

(a)

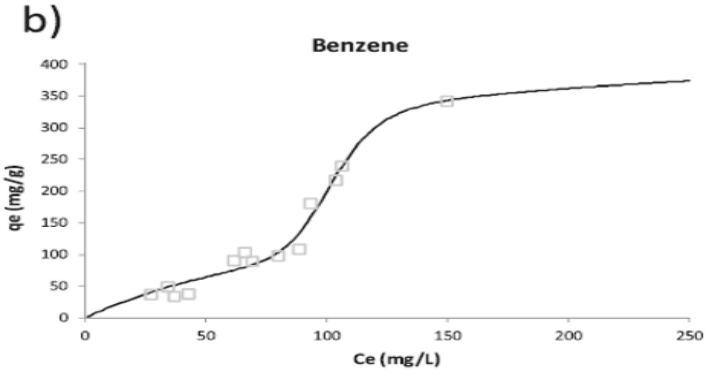

(b)

Figure 18. Toluene and benzene adsorption isotherms upon CMK-3.

$$q_e = q_{\max}.\left(\frac{K1.Ce}{1+K1.Ce}+\frac{Ks.(Ce)^n}{1+Ks.(Ce)^n}\right) \quad \textbf{(4)}$$

where Ce is the equilibrium solution concentration in mg/L, Kl is the Langmuir constant, qe is the adsorbed quantity of toluene or benzene in mg/g, and qmax is the maximum adsorbable quantity in mg/g.

Ks the Langmuire-Freundlich constant in L/g, and n is a general quantity that denotes the adsorption mechanism's heterogeneity.

The Langmuir model indicated that the first stage in the adsorptions of toluene and benzene from liquid phase onto CMK-3would be adsorption on the mesoporous channel wall until a monolayer was achieved Figure 18. Following the creation of the first monolayer, the adsorption of hydrocarbon compounds proceeded to produce subsequent layers until the entire mesoporous channel was filled. Latter procedure matched the experimental isotherms' second stage. The optimized parameters derived from nonlinear regressions of the data using the Lee model (4) are displayed in Table 6. In the Langmuir and Langmuire-Freundlich domains, toluene showed the strongest affinity (the highest values of Kl and Ks, respectively). The methyl group in toluene, which was missing from the benzene molecule, may have contributed to its higher affinity. While the benzene ring, which lacked a substituent, was free to go in any direction, the toluene molecule's ability to freely rotate in the space may be restricted by this methyl group. Benzene may have had a reduced affinity for CMK-3 due to its higher mobility. Accordingly, a more sterically hindered molecules, like toluene, adsorbed more readily than mobile molecules, like benzene [23,24]. Instead, benzene had a higher qmax value than toluene, most likely as a result of the molecule's smaller size, which let more aromatic ring to stack inside the CMK-3's pore. These findings, demonstrate how well the CMK-3 removes aromatic compounds from tainted water.

Table 6. Toluene and Benzene adsorption onto CMK-3 with optimised adsorption parameters.

Parameters	Benzene	Toluene
Ks (L/mg)	0.0368 ± 0.0004	0.0976 ± 0.0006
Kl (L/mg)	0.0076 ± 0.0027	0.0307 ± 0.0089
qmax (mg/g)	356± 27	412 ± 38
N	12.41 ± 3.92	11.25 ± 1.97
R^2	0.953	0.951

4. Conclusion

The present study has compared the adsorption capacities of synthetic clinoptilolite, synthetic Purolite, and mesoporous carbon CMK-3 as to the removal of heavy metals (Pb^{2+}, Cd^{2+}, Ni^{2+}) and organic pollutants (benzene and toluene) in real petrochemical effluent sample taken in the Al-Dora Refinery of Baghdad, Iraq. Introduction of practical industrial effluent in experiment during the laboratory testing combines a more ideal measurement of the adsorbent functioning in the studious environment of complex contamination and salinity.

The kinetic findings were that clinoptilolite and Purolite had high affinity in adsorbing metal ions and they attained equilibrium within 100 minutes as opposed to CMK-3 which took a much longer period of time to reach the equilibrium. Purolite gave the maximum affinity till the metal species whereas clinoptilolite was selective to Pb^{2+}. CMK-3 is less effective on the removal of metal but its performance was excellent in the removal of hydrocarbons; more than 80 percent of both benzene and toluene were removed in 7 hours.

The studies resulted in isotherms and it was found that the Purolite and clinoptilolite adsorbed LangmuirFreundlich and that CMK-3 was of Henry-type and followed a multilayer Swedish petroleum industry metal so following a two-step hybrid isotherm was found to resemble the behavior of hydrocarbons. Significantly, it was observed that an ionic strength of 0.1mol L-1 in the Purolite was more effective than the clinoptilolite.

In concluding, it was determined that the presence of benzene increased the adsorption of Pb^2 2 to both Purolite and clinoptilolite thereby indicating the possible complexation between Pb and benzene, and decreased uptake of Cd^2 2 and Ni^2 2. This effect coupled with high affinity of CMK-3 towards aromatic hydrocarbons strengthens the significance of using materials that can effectively cope with the co-contaminated conditions.

On the whole, CMK-3 proves to be a rather good candidate of organic contaminants clean up, in particular in systems having volatile aromatics abundance, and Purolite and clinoptilolite are still excellent heavy metals remedial agents.

Future studies should explore the functionalization of mesoporous carbon materials to enhance metal adsorption, as well as the regeneration and reuse of all adsorbents in continuous flow systems.

This research provides critical insights into material selection for industrial effluent treatment and highlights the practical relevance of combining synthetic materials with real effluent testing to develop more resilient, scalable, and environmentally robust treatment technologies.

References

[1] Jeong, Y., Cui, M., Choi, J., Lee, Y., Kim, J., Son, Y., & Khim, J. (2020). Development of modified mesoporous carbon (CMK-3) for improved adsorption of bisphenol-A. *Chemosphere, 238,* 124559. https://doi.org/10.1016/j.chemosphere.2019.124559

[2] Alsawalha, M. (2019). Overview of current and future perspectives of Saudi Arabian natural clinoptilolite zeolite: A case review. *Journal of Chemistry, 2019,* 3153471. https://doi.org/10.1155/2019/3153471

[3] Phan, T. N., Gong, M. K., Thangavel, R., Lee, Y. S., & Ko, C. H. (2019). Enhanced electrochemical performance for EDLC using ordered mesoporous carbons (CMK-3 and CMK-8): Role of mesopores and mesopore structures. *Journal of Alloys and Compounds, 780,* 90–97. https://doi.org/10.1016/j.jallcom.2018.11.265

[4] Bożęcka, A. M., & Sanak-Rydlewska, S. (2018). The use of ion exchangers for removing cobalt and nickel ions from water solutions. *Archives of Mining Sciences, 63*(3), 689–704. https://doi.org/10.24425/ams.2018.124981

[5] Kalash, K. R., & Albayati, T. M. (2021). Remediation of oil refinery wastewater implementing functionalized mesoporous materials MCM-41 in batch and continuous adsorption process. *Desalination and Water Treatment, 220,* 130–141. https://doi.org/10.5004/dwt.2021.27107

[6] Li, S., Huang, L., Wang, D., Zhou, S., Sun, X., Zhao, R., … Chen, R. (2023). A review of 3D superhydrophilic porous materials for oil/water separation. *Separation and Purification Technology, 319,* 124847. https://doi.org/10.1016/j.seppur.2023.124847

[7] Favvas, E. P., Tsanaktsidis, C. G., Sapalidis, A. A., Tzilantonis, G. T., Papageorgiou, S. K., & Mitropoulos, A. C. (2016). Clinoptilolite, a natural zeolite material: Structural characterization and performance evaluation on its dehydration properties of hydrocarbon-based fuels. *Microporous and Mesoporous Materials, 225,* 385–391. https://doi.org/10.1016/j.micromeso.2016.01.036

[8] Silva, R. A., Zhang, Y., Hawboldt, K., & James, L. A. (2021). Study on iron-nickel separation using ion exchange resins with different functional groups for potential iron sub-production. *Mineral Processing and Extractive Metallurgy Review, 42*(2), 75–89. https://doi.org/10.1080/08827508.2019.1702061

[9] Huang, H., Cai, Y., Zhao, C., Chen, Z., Liao, Z., Xie, H., … Li, D. (2024). Fabrication of 3D porous materials with underliquid dual superlyophobic properties for oil–water emulsion separation and Cu2+ adsorption. *Separation and Purification Technology, 339,* 126691. https://doi.org/10.1016/j.seppur.2024.126691

[10] Wu, R., Ye, Q., Wu, K., & Dai, H. (2021). Potassium-modified ordered mesoporous carbon materials (K-CMK-3): Highly efficient adsorbents for NO adsorption at low temperatures. *Journal of Solid State Chemistry, 294,* 121844. https://doi.org/10.1016/j.jssc.2020.121844

[11] Shao, Z. D., Zhang, Q. J., Zheng, Y. M., & Cheng, X. (2024). A novel pearls-like hierarchical porous silica aerogel monolith for efficient oil/water separation. *Journal of Porous Materials, 31,* 1–11. https://doi.org/10.1007/s10934-024-01491-3

[12] Song, Y., Phipps, J., Zhu, C., & Ma, S. (2023). Porous materials for water purification. *Angewandte Chemie International Edition, 62,* e202216724. https://doi.org/10.1002/anie.202216724

[13] Kumar, A., Naidu, G., Fukuda, H., Du, F., Vigneswaran, S., Drioli, E., & Lienhard, J. H. (2021). Metals recovery from seawater desalination brines: Technologies, opportunities, and challenges. *ACS Sustainable Chemistry & Engineering, 9*(23), 7704–7712. https://doi.org/10.1021/acssuschemeng.1c01463

[14] Vorokhta, M., Morávková, J., Dopita, M., Zhigunov, A., Šlouf, M., Pilař, R., & Sazama, P. (2021). Effect of micropores on CO_2 capture in ordered mesoporous CMK-3 carbon at atmospheric pressure. *Adsorption, 27*(8), 1221–1236. https://doi.org/10.1007/s10450-021-00313-8

[15] Liou TH, Lai BC, Xu XY. High-quality Carbons Mesostructured from Korea (CMK)-type carbons with adjustable mesostructure used as potential nanoadsorbent for enhanced tannic acid capture. Desalination. 2025 Dec 3:119725.

[16] de Castro-Alves L, Yánez-Vilar S, González-Goméz MA, Garcia-Acevedo P, Arnosa-Prieto Á, Pineiro-Redondo Y, Rivas J. Understanding adsorption mechanisms and metal ion selectivity of superparamagnetic beads with mesoporous CMK-3 carbon and commercial activated carbon. Microporous and Mesoporous Materials. 2024 Jun 15;374:113159.

[17] Al-Ghouti, M. A., & Da'ana, D. A. (2020). Guidelines for the use and interpretation of adsorption isotherm models: A review. *Journal of Hazardous Materials, 393,* 122383. https://doi.org/10.1016/j.jhazmat.2020.122383

[18] Wang, J., & Guo, X. (2020). Adsorption isotherm models: Classification, physical meaning, application and solving method. *Chemosphere, 258,* 127279. https://doi.org/10.1016/j.chemosphere.2020.127279

[19] Kundu, P., & Mishra, I. M. (2018). Treatment and reclamation of hydrocarbon-bearing oily wastewater as a hazardous pollutant by different processes and technologies: A state-of-the-art review. *Reviews in Chemical Engineering, 35*(1), 73–108. https://doi.org/10.1515/revce-2017-0034

[20] Shao, J., Zhao, Y., Li, D., Xu, S., Dou, Z., Sun, Z., … Zhou, Y. (2022). Synthesis and characterization of superhydrophobic fluorinated mesoporous silica for oil/water separation. *Microporous and Mesoporous Materials, 344,* 112240. https://doi.org/10.1016/j.micromeso.2022.112240

[21] Dashtpeyma, G., & Shabanian, S. R. (2023). Efficient photocatalytic oxidative desulfurization of liquid petroleum fuels under visible-light irradiation using a novel ternary heterogeneous BiVO4-CuO/modified natural clinoptilolite zeolite. *Journal of Photochemistry and Photobiology A: Chemistry, 445,* 115024. https://doi.org/10.1016/j.jphotochem.2023.115024

[22] Dinari, S., & Eslami, F. (2020). Effect of clinoptilolite natural zeolite particles on the destabilization of the oil-in-water emulsion. *Colloid and Interface Science Communications, 37,* 100297. https://doi.org/10.1016/j.colcom.2020.100297

[23] Kiomarsipour, N., Alizadeh, M., Alizadeh, M., & Ghani, K. (2021). Synthesis and surface-functionalizing of ordered mesoporous carbon CMK-3 for removal of nitrate from aqueous solution as an effective adsorbent. *Diamond and Related Materials, 116,* 108419. https://doi.org/10.1016/j.diamond.2021.108419

[24] Liu, T., & Chen, J. (2021). Extraction and separation of heavy rare earth elements: A review. *Separation and Purification Technology, 276,* 119263. https://doi.org/10.1016/j.seppur.2021.119263